



Article scientifique

Article

2013

Published version

Open Access

This is the published version of the publication, made available in accordance with the publisher's policy.

Oxazinoindolines as Fluorescent H⁺ Turn-On Chromoionophores For Optical and Electrochemical Ion Sensors

Xie, Xiaojiang; Crespo Paravano, Gaston Adrian; Bakker, Eric

How to cite

XIE, Xiaojiang, CRESPO PARAVANO, Gaston Adrian, BAKKER, Eric. Oxazinoindolines as Fluorescent H⁺ Turn-On Chromoionophores For Optical and Electrochemical Ion Sensors. In: Analytical chemistry, 2013, vol. 85, n° 15, p. 7434–7440. doi: 10.1021/ac401367b

This publication URL: <https://archive-ouverte.unige.ch/unige:31510>

Publication DOI: [10.1021/ac401367b](https://doi.org/10.1021/ac401367b)

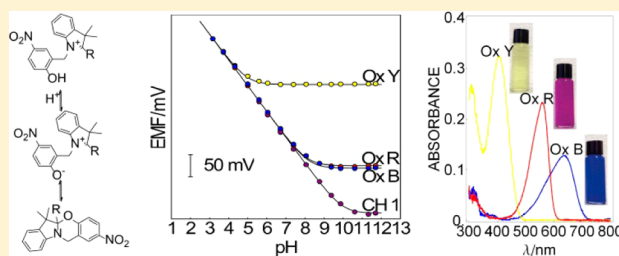
Oxazinoindolines as Fluorescent H⁺ Turn-On Chromoionophores For Optical and Electrochemical Ion Sensors

Xiaojiang Xie, Gastón A. Crespo, and Eric Bakker*

Department of Inorganic and Analytical Chemistry, University of Geneva, Quai Ernest-Ansermet 30, CH-1211 Geneva, Switzerland

Supporting Information

ABSTRACT: We propose here a new class of fluorescent H⁺ turn-on oxazinoindoline (Ox) dyes as chromoionophores suitable for the development of polymeric ion-selective membranes. Through rational design, oxazinoindolines with varying basicities and tunable absorption bands that extend to the near-infrared region were prepared. The basicities of the compounds were evaluated by potentiometry and fluorescence spectroscopy. By comparing the potentiometric lower detection limit with chromoionophore I (pK_a = 14.80 ± 0.03 in PVC-NPOE), pK_a values were determined for Ox Y, Ox R, and Ox B to be 9.80 ± 0.03, 12.85 ± 0.03, and 12.95 ± 0.03, respectively. Unlike conventional pH indicators that involve only a protonated and deprotonated form, a third species, arising from the thermal isomerization of the Ox compounds in polar solvents, may influence the overall protonation equilibrium. Interestingly, this results in an apparent pK_a increase in the fluorescence mode when more polar PVC–NPOE membranes were utilized. The isomerization is suppressed in nonpolar PVC–DOS membranes. Na⁺-selective optical sensors were successfully prepared using the Ox dyes as an early application of the compounds in ion-selective optical sensors. The compounds were also successfully evaluated in a dynamic electrochemistry (chronopotentiometry) sensing mode for the detection of total alkalinity.



Chromoionophores are lipophilic pH indicators that are essential components of modern ion-selective optical sensors.^{1–4} These sensors often contain additionally a lipophilic receptor for the analyte ion, also called ionophore and an ion-exchanger. The simultaneous existence of a chromoionophore and analyte-selective ionophore results in a sensing mechanism that relies on a competition (for cationic analytes) or cooperation (for anions) between the analyte and H⁺ in the sample.⁵ Here, H⁺ functions as a reference ion in the sensing film so that the change in the analyte concentration also alters the concentration of H⁺ in the membrane, which in turn changes the optical properties of the chromoionophore.

Today, most commercially available chromoionophores are derivatives of Nile blue, such as chromoionophore I (CH 1) and a number of other structurally similar analogues.⁶ Despite numerous reports for pH-sensitive dyes in aqueous solutions or organic solvents, Nile blue derivatives are still predominantly used in ion-selective optical sensors.⁷ CH 1 was first developed by the group of Simon in 1989 for use in a calcium-selective optode.⁸ Soon afterward, pH electrodes and optical sensors selective for ammonium, Pd²⁺, and K⁺ based on this compound were reported.^{9–12} Structure modification provides the opportunity to tune the pK_a values of the Nile blue derivatives. Still, the available basicity range is limited, and the synthesis can be challenging.¹³ Moreover, the spectra of these compounds are quite similar and lack variation since they belong to the same family. Lipophilic derivatives of fluorescein, such as chromoionophore VI and XI, are also used for anion-selective sensors.^{14,15} Other types of compounds that belong to the

azobenzene and stilbene families, such as chromoionophore IV, X, and IX are also used for ion-selective sensors; however, they are not fluorescent, and thus their application is limited.^{16,17} There is still an urgent need to expand the available palette of chromoionophores for sensing applications.

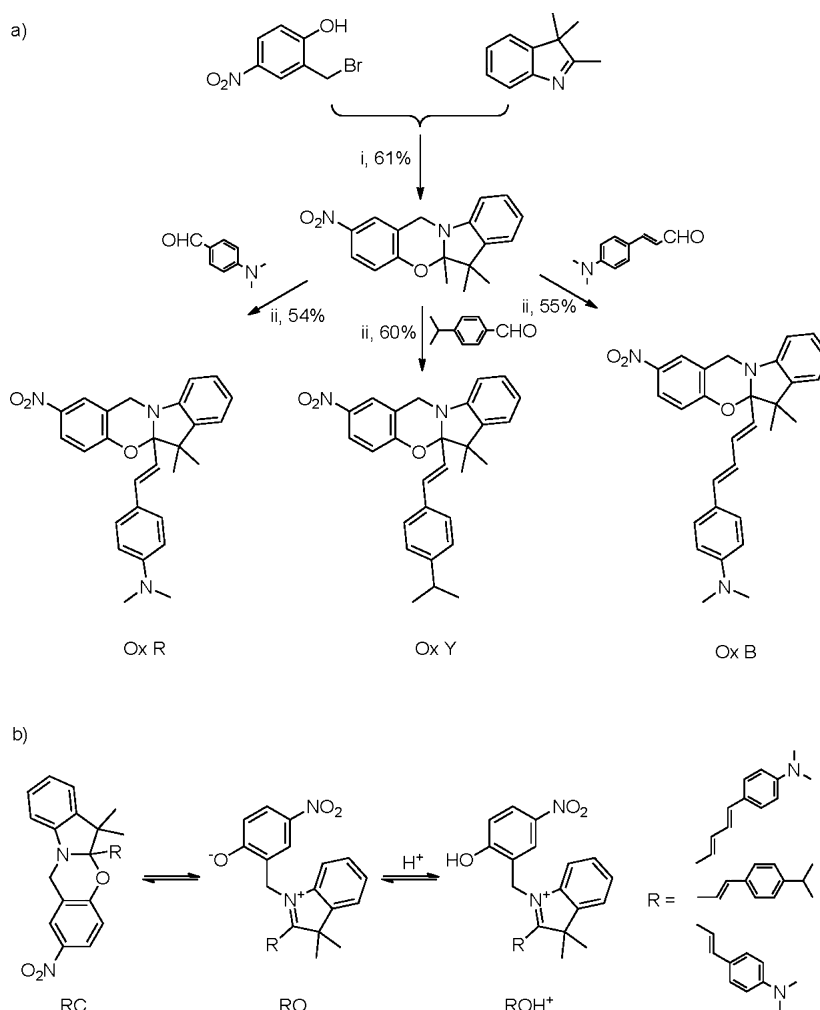
The spectrum of the chromoionophore normally acts as the signal output, and a preferred type of signaling is the fluorescent “turn-on” type. This results in an important contrast with the background, which is important in fluorescence microscopy.¹⁸ There have been many reports on fluorescent turn-on sensors in aqueous or organic phase for various ions such as Zn²⁺, Cu²⁺, Hg²⁺, and others,^{19–22} but membrane-based sensors of this type have not been frequently reported.^{23–25}

We have observed that oxazinoindolines (Ox), a class of compounds initially reported for photoswitches,^{26–29} are very sensitive to pH changes. Here, through rational design, oxazinoindolines with tunable pK_a values and variable emission wavelengths that extend to the near-infrared region were synthesized. These compounds may exist in a ring-closed (RC) or a ring-opened (RO) form. The ring-opened form is strongly colored and more basic, while the ring-closed form is colorless and much less basic. Therefore, the acid–base reaction is dominated not only by the protonated and deprotonated form,

Received: May 6, 2013

Accepted: June 24, 2013

Published: June 24, 2013

Scheme 1. (a) Synthetic Route for the Oxazinoindoline Dyes;^a (b) Thermal Isomerization Reaction for Oxazinoindoline and Protonation of the Ring-Opened Form

^aReagents and conditions: (i) acetonitrile, room temperature, 12 h; (ii) ethanol, reflux, N₂, 12 h.

as in classical pH indicators but also by a third species that arises from thermal isomerization. This gives rise to a substantially different apparent basicity when interrogated by potentiometry or spectroscopy. Ion-selective liquid membranes were prepared from these compounds and were characterized with different techniques including potentiometry, fluorescence spectrometry, and chronopotentiometry. The basicity of these compounds was quantified by comparison with chromoionophore I (CH 1). The results suggest that these oxazinoindoline compounds form promising candidates as a new family of chromoionophores for polymeric ion-selective systems.

EXPERIMENTAL SECTION

Reagents. Poly(vinyl-chloride) (PVC, high molecular weight), bis(2-ethylhexyl) sebacate (DOS), 2-nitrophenyl octyl ether (NPOE), sodium ionophore X, potassium tetrakis-[3,5-bis(trifluoromethyl)phenyl]borate (KTFPB), 2-amino-2-hydroxymethyl-propane-1,3-diol (Tris), chromoionophore I, acetic acid (HA), sodium chloride (NaCl), fluorescein, rhodamine B, cryptocyanine, and tetrahydrofuran (THF) were obtained from Sigma-Aldrich. Oxazinoindolines were synthesized according to synthesis of similar compounds in previous reports.²⁸ (See Supporting Information for structural

information.) All buffer solutions were prepared by dissolving appropriate salts into deionized water (Mili-Q). All solvents and reagents used were analytically pure unless otherwise specified.

Membranes. The membranes for potentiometric measurements were prepared by dissolving 150 mg of the mixture composed of 0.002 mmol of Ox or CH 1, 0.55 mmol (0.5 mg) of KTFPB, 50 mg of PVC, and 100 mg NPOE or DOS in 2 mL of THF. The cocktail solution was then poured into a glass ring (22 mm in diameter), placed on a slide glass, and dried overnight at room temperature under a dust-free environment. Small disks were punched from the cast films and mounted in Ostec electrode bodies (Ostec, Sargans, Switzerland).

When porous polypropylene (PP) membranes (Celgard, 0.237 cm² in surface area, 25 μm in thickness, and kindly provided by Membrana Wuppertal, Germany) were used as supporting material, the same amount of KTFPB, Ox, or CH 1 was dissolved in 90 mg of NPOE. For chronopotentiometric measurements, the organic cocktail contains 120 mmol kg⁻¹ of Ox or CH 1, 60 mmol kg⁻¹ of KTFPB, 90 mmol kg⁻¹ of ETH 500, and 190 mg of NPOE. The membranes were soaked in THF for 10 min to remove any possible contaminants. When the membrane was found to be completely dry, 3 μL (large

excess) of the cocktail solution was deposited on it. The impregnation of the cocktail was found to be instantaneous; however, the membrane was let in the Petri dish for ca. 10 min to ensure a homogeneous and reproducible impregnation of the pores. Afterward, the membrane was conditioned in the buffer solution for 40 min. Finally, the membrane was mounted in the Ostec electrode body.

For the optical sodium-selective membrane, 0.002 mmol of Ox or CH 1, 0.002 mmol of KTFPB, 0.005 mmol of sodium ionophore X, 32 mg of PVC, and 64 mg of NPOE were dissolved in 1 mL of THF. Likewise, for the pH optode, 0.001 mmol of Ox, 0.001 mmol of KTFPB, 32 mg of PVC, and 64 mg of NPOE were dissolved in 1 mL of THF. A thin film was formed by drop casting 50 μL of the cocktail onto a quartz disk with a diameter of 35 mm and evaporating the solvent for 30 min. The quartz disk was then mounted onto a previously described flow cell³⁰ for spectroscopic measurements.

Instrumentation and Measurements. The glass pH electrode with combined Ag/AgCl reference (Ecotrode Plus) and a double-junction Ag/AgCl/3 M KCl/1 M LiOAc reference electrode were purchased from Metrohm (Metrohm-Toledo AG, Schwerzenbach, Switzerland). The potentiometric sensor responses are measured with an EMF-16 precision electrochemistry EMF interface from Lawson Laboratories Inc. Chronopotentiometric measurements were performed with an Autolab PGSTAT302N (MULTI 16 module, Metrohm Autolab, Utrecht, The Netherlands) that allows one to read up to 16 working electrodes placed in the same electrochemical cell. A Faraday cage was used to protect the system from undesired noise.

The absorbance was measured with a UV-vis spectrometer (SPECORD 250 plus, Analytic Jena, AG, Germany), and fluorescence was measured with a fluorescence spectrometer (Fluorolog3, Horiba Jobin Yvon). For fluorescent pH and Na^+ calibration, excitation wavelength of 410, 478, 660, and 600 nm was chosen for Ox Y, Ox R, Ox B, and CH 1, respectively, while the emission at 520, 605, 720, and 700 nm was monitored. The excitation light was guided with a liquid waveguide onto the surface of the quartz disk in the flow cell, and the emission light was collected from the same end. The membrane was in contact with aqueous solution in which the pH or Na^+ concentration was adjusted. The sample solution was circulated through the flow cell with a peristaltic pump (Gilson Miniplus 3). The excitation slit was set at 3 nm for all measurements. The apparent degree of protonation ($1 - \alpha^*$) was calculated according to eq 1 in Supporting Information.

RESULTS AND DISCUSSION

Three oxazinoindoline derivatives, labeled here as Ox Y, Ox R, and Ox B, have been synthesized in two facile steps from commercial starting materials, as shown in Scheme 1a. Compared to the established Nile blue family of chromoionophores, the synthesis is much less cumbersome, and the yields are attractive. The details of the synthesis and the structural information can be found in the Supporting Information. The ring-opening/closing isomerization reaction (Scheme 1b) is a thermally driven process and can, in some cases, be achieved through UV irradiation, making oxazinoindolines photochromic compounds.²⁶ The photoswitching behavior depends on the chemical structure, and no photochromic effect was observed for the compounds reported here. The ring-opened (RO, see Scheme 1) and the ring-closed (RC) form should differ in basicity since the RO form possesses a phenolate group that is

absent in the RC form. Therefore, the compounds are pH-sensitive, and the equilibrium state of the reaction can be shifted with hydrogen ions.

The RO form is colored owing to the extended conjugation in the merocyanine moiety of the molecule and results in absorbance in the visible range. However, the RC form does not show any absorption region in the visible range with the exception of Ox R. Slight maxima at 424 and 552 nm that belong to the 4-nitrobenzophenolate and the merocyanine moieties, respectively, were observed in acetonitrile, indicating that in such environment, the existence of the RO form is not negligible (see Figure S1 in Supporting Information). The absorption and emission spectra are shown in Figure 1. The

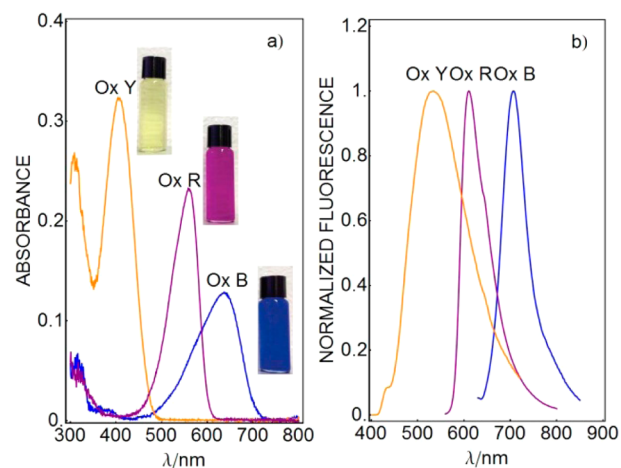


Figure 1. (a) Absorbance spectra for Ox Y (5×10^{-5} M), Ox B (5×10^{-6} M), and Ox R (5×10^{-6} M) in acetonitrile with 10 equiv of trifluoroacetic acid. Insets: photographs of the corresponding solutions. (b) Normalized fluorescence emission spectra for 5×10^{-5} M of the three Ox compounds in acetonitrile with 10 equiv of trifluoroacetic acid.

absorption maxima for Ox Y, Ox R, and Ox B were found at 409 nm ($\epsilon = 1.6 \times 10^4 \text{ L mol}^{-1} \text{ cm}^{-1}$), 558 nm ($\epsilon = 1.2 \times 10^5 \text{ L mol}^{-1} \text{ cm}^{-1}$), and 637 nm ($\epsilon = 6.4 \times 10^4 \text{ L mol}^{-1} \text{ cm}^{-1}$). Compared with Ox R, the addition of one more double bond (Ox B) red-shifted the absorption maximum by 79 nm and the emission maximum by 100 nm in acetonitrile. In contrast, Ox Y showed a blue shift of 149 nm in the absorption maximum and 78 nm in emission maximum. The blue shift was caused by the replacement of the *N,N*-dimethylamino group on the benzene ring to the isopropyl group. This replacement reduces the electron push-pull effect on the absorbance of the RO form since the isopropyl group is a less effective electron donor than the *N,N*-dimethylamino group. It is worth mentioning that the absorption and emission of Ox B has reached the near-infrared region, which is advantageous in biological imaging since the excitation and emission at this region will cause much less background interference. The quantum yield of these compounds was determined in ethanol to be 0.12, 0.04, and 0.01 for Ox B, Ox R, and Ox Y respectively, using cryptocyanine, rhodamine B, and fluorescein as references.

The oxazinoindoline dyes were incorporated into NPOE plasticized PVC membranes and polypropylene membranes for the fabrication of potentiometric pH-selective electrodes. In order to estimate the $\text{p}K_a$ values, CH 1 was selected as a reference compound. The $\text{p}K_a$ value of CH 1 was reported to be 14.80 ± 0.03 ¹³ in PVC-NPOE, and by comparing the

unbiased detection limits at high pH, one can quantify the pK_a values. For this purpose, the pH response of the electrodes was measured in a buffer solution containing 0.01 M of tetramethylammonium (TMA⁺) chloride as interfering ion that, owing to its symmetrical structure, is expected not to chemically interact with any of the dyes. The experimentally observed response curves are shown in Figure 2 (see Figure S2 in Supporting Information for the pH response of the corresponding supported polypropylene membrane based electrodes).

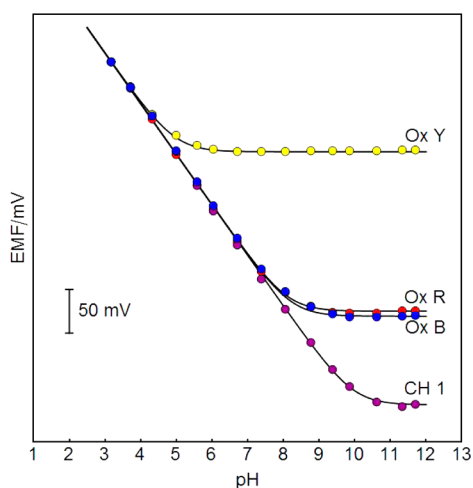


Figure 2. Potentiometric pH response for PVC–NPOE-based electrodes based on one of the three oxazinoindoline derivatives or CH 1 as chromoionophore. The pH of the buffer solution (2.5 mM NaH₂PO₄, 2.5 mM boric acid, 2.5 mM citric acid, 0.1 M NaCl, and 0.01 M TMA⁺Cl⁻) was adjusted by addition of 1 M NaOH solution. The solid line was calculated from the Nicolsky–Eisenman equation.

The lipophilic TMA⁺ cation acted as a strong interference here, so that the detection limit at high pH can be observed in all cases. Without such strong interference, even with 0.1 M NaCl as a background, a Nernstian response was obtained over the whole buffer range, making the detection limits too difficult to determine. The pK_a values were extracted from the lower detection limit for H⁺ using eq 1, where pH(LDL) and pH(LDL,CH1) are the pH values at the lower detection limit for a membrane containing the dye of interest and CH 1, respectively.⁵

$$pK_a - pK_a(\text{CH 1}) = \text{pH}(\text{LDL}) - \text{pH}(\text{LDL,CH 1}) \quad (1)$$

This equation should be valid for membranes of otherwise identical composition. Figure 2 shows the potentiometric calibration curves from which the pK_a values were extracted for Ox Y, Ox R, and Ox B as 9.80 ± 0.03 , 12.85 ± 0.03 , and 12.95 ± 0.03 , respectively. Note that the basicity of Ox Y is particularly low compared with the others. This difference is a consequence of the replacement of the *N,N*-dimethylamino group in Ox R and Ox B with the isopropyl group in Ox Y. The presence of the nitrogen atom enables Ox R and Ox B to exist in resonance structures and brings additional stabilization to the RO form, while for Ox Y, resonance structures cannot be formed (see Figure S3 in Supporting Information).

In the next step, optically responsive pH-sensitive films containing the compounds were prepared (see membrane composition above). The pH response was re-evaluated in the same buffer solution using fluorescence emission as signal

output. The emission intensity at the emission maximum was monitored during the experiment. Under this operating mode, the Ox compounds exhibited an advantage since the emission intensity change at the maximum emission wavelength was larger than for CH 1.

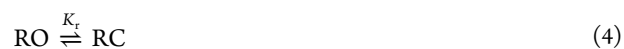
One should note that for CH 1 only the protonated form and the deprotonated form are involved in the optode response:



For oxazinoindoline dyes, on the other hand, three forms, namely, the RC, RO, and the protonated ring-opened form ROH⁺, are potentially important, with K_a the acid dissociation constant in the membrane (note that the ring-closed form is used here as the conjugate base):



The isomerization equilibrium between nonprotonated RO and RC form is given as



Because of the possible presence of the RO species, the fluorescence intensity was taken to calculate a $1 - \alpha^*$ value (see Supporting Information). Consequently, the $1 - \alpha^*$ value, meaning the mole fraction of the protonated form, depends on both the basicity of RO (K_a) and the thermal equilibrium between RC and RO (K_r). The response function of a pH-sensitive optode containing Ox B and KTFPB in the presence of a monovalent interfering ion can be derived from charge and mass balances, the ion-exchange equilibrium, and the chemical equilibria shown in eqs 3 and 4 (see Supporting Information for details) to give

$$a_{\text{H}^+}^{\text{aq}} = a_{\text{J}^+}^{\text{aq}} K_a K_{\text{ex}} \frac{1 + K_r}{K_r} \frac{1 - \alpha^*}{\alpha^*} \frac{1}{(1 - \alpha^*) \text{Ind}_T - R_T} \quad (5)$$

where $a_{\text{H}^+}^{\text{aq}}$ and $a_{\text{J}^+}^{\text{aq}}$ are the activities of H⁺ and the interfering ion (TMA⁺ or Na⁺) in aqueous solution, Ind_T and R_T are the total concentration of Ox B and KTFPB, and K_{ex} is the exchange constant for the so-called free hydrogen and interfering ions. The observed optical pH response is shown in Figure 3 where the solid lines are theoretical fittings

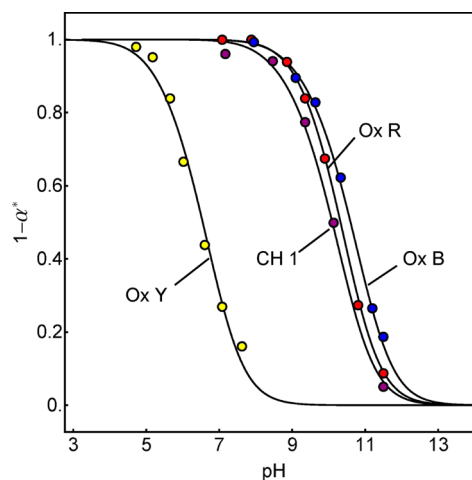


Figure 3. Optode pH response for films containing Ox dyes or CH 1 as chromoionophore, as indicated, without additional cation-selective ionophore. The same buffer solution as for Figure 2 was used.

according to eq 5. From the optode response, one can predict the theoretical potentiometric response. The correlation between the optode response and the potentiometric response (Figure 2) can be established by considering the free proton concentration in the membrane ($a_{\text{H}^+}^{\text{m}}$), as shown in eq 6. The potential (EMF) in Figure 2 measured under the same conditions can then be expressed by eq 7, where s is the Nernstian slope and E^0 a constant.

$$a_{\text{H}^+}^{\text{m}} = \frac{K_a(K_r - (1 + K_r)\alpha^*)}{\alpha^*K_r} \quad (6)$$

$$\begin{aligned} \text{EMF} &= E^0 + s \log \frac{a_{\text{H}^+}^{\text{aq}}}{a_{\text{H}^+}^{\text{m}}} \\ &= E^0 \\ &\quad + s \log \frac{(1 - \alpha^*)a_{\text{H}^+}^{\text{aq}}K_{\text{ex}}(1 + K_r)}{(\alpha^* + (\alpha^* - 1)K_r)((\alpha^* - 1)\text{Ind}_T + R_T)} \end{aligned} \quad (7)$$

The correlation between the optical response and potentiometric response for a PVC–NPOE membrane containing Ox B is presented in Figure 4a. The solid line is the theoretical

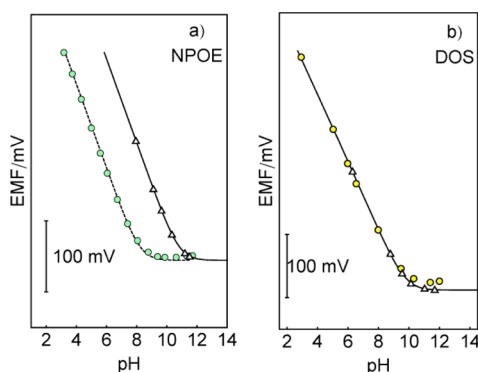


Figure 4. Correlation between the potentiometric pH response and optode pH response for membrane using Ox B as chromoionophore (a) in PVC–NPOE and (b) in PVC–DOS. The solid lines and triangles are calculated according to eq 7 with constants obtained from Figure 3 and Figure S7 in Supporting Information. The dashed line is a shift of the solid line in panel a to the left by 2.6 units to fit the potentiometric data. The circles are experimentally measured potentiometric responses.

potentiometric response curve calculated according to eq 7 using K_a , K_r , and K_{ex} values obtained from the corresponding optical calibration curve (Figure 3). As shown in Figure 4 a, in PVC–NPOE, the measured data differed from the theoretical curve by 2.6 units. The oxazinoindoline compounds exhibit an apparently higher basicity than CH 1 in fluorescent mode, which seemingly contradicts the potentiometric data in Figure 2, which had suggested a lower basicity for all oxazinoindolines relative to CH 1.

This unusual discrepancy is perhaps partly explained by the presence of the RO species in the optode equilibrium. The fluorescence and absorbance spectra of pH sensitive films containing the Ox dyes are measured and shown in Figures S4 and S5 in Supporting Information. Comparing the emission intensity at high and low pH conditions where the RO form of Ox dyes should be completely deprotonated and protonated, it is clear that in a polar environment, such as PVC–NPOE, the

formation of the zwitterionic species may be preferred relative to the RC form. The concentration of RC is reduced relative to all unprotonated indicators, thereby diminishing the apparent basicity of the dye. This perhaps explains the poorer selectivity of the ion-selective electrode toward the interfering ion. In agreement with theoretical expectations (see Figure S7 in Supporting Information) where the zwitterion is preferred in a polar environment such as PVC–NPOE, the potentiometric low detection limit for H^+ shifted to lower pH. The formation of the zwitterionic RO form in nonpolar PVC–DOS should be suppressed compared with the polar PVC–NPOE since it is less preferred in nonpolar environment. The dependence of such entropy-driven thermal isomerization on microenvironments, such as solvents, for compounds with similar structure has been reported before.³¹

To confirm, the pH response for a PVC–DOS membrane containing Ox B was also measured, and the correlation between the optical response (see Figure S7 in Supporting Information) and potentiometric response is presented in Figure 4b. In PVC–DOS, the chromoionophore is expected to more closely function as a typical two-component system (in analogy to CH 1) due to the suppression of the thermal ring-opening reaction, and a good correlation was indeed observed.

A Na^+ -selective optode was prepared with Ox B and Ox R as an early example of a fluorescent ion sensor. Ox Y was not tested due to its relatively low $\text{p}K_a$. Selectivity for Na^+ was assured by addition of sodium ionophore X to the sensing film. Here, H^+ and Na^+ in the sample will compete with each other for extraction into the optode film and hence, with a constant hydrogen ion background, the concentration of Na^+ alters the fluorescence output. Figure S8 in Supporting Information shows the calibration curves for the sensors in 0.01 M Tris–HCl buffer at pH 7.2. The results were compared with a conventional CH 1 based Na^+ -selective optode, and the calibration curves are consistent with the basicity tendency displayed in Figure 3. Again, the signal-to-noise ratio was better for the Ox dyes than CH 1 since the Ox dyes exhibit a larger emission intensity variation at their emission maxima (see Figure S9 in Supporting Information).

CH 1 has been recently incorporated in chronopotentiometric sensors to determine total alkalinity and total acidity *in situ* in artificial samples.³² Here, Ox B and Ox R were also evaluated as potential proton ionophore candidates under electrodynamic conditions. A sequence of galvanostatic and potentiostatic pulses allows one to achieve dynamic electrochemistry perturbations between the membrane and sample interface.³³ For instance, if an anodic pulse is applied, protons are released from the membrane to the sample. When a base is present, it will become protonated near the electrode surface. While the proton flux is constant, the flux of this base from the solution bulk to the electrode membrane can only be maintained up to a transition time (τ), after which time the proton flux can no longer be maintained, and the resulting phase boundary pH change gives rise to an observed potential change. The transition time is visualized as the maximum of the time derivative of the potential as shown in Figure 5 (see Figure S10 in the Supporting Information for raw data of E vs time). By increasing the concentration of Tris at a constant applied current, the transition times move to larger values, in quantitative agreement with the Sand equation. The diffusion coefficient of Tris in aqueous phase is obtained from the linear plot of $\tau^{0.5}$ vs $[\text{Tris}]$ for each individual dye. The estimated diffusion coefficients for Tris are $(6.59 \pm 0.05) \times 10^{-6} \text{ cm}^2 \text{ s}^{-1}$

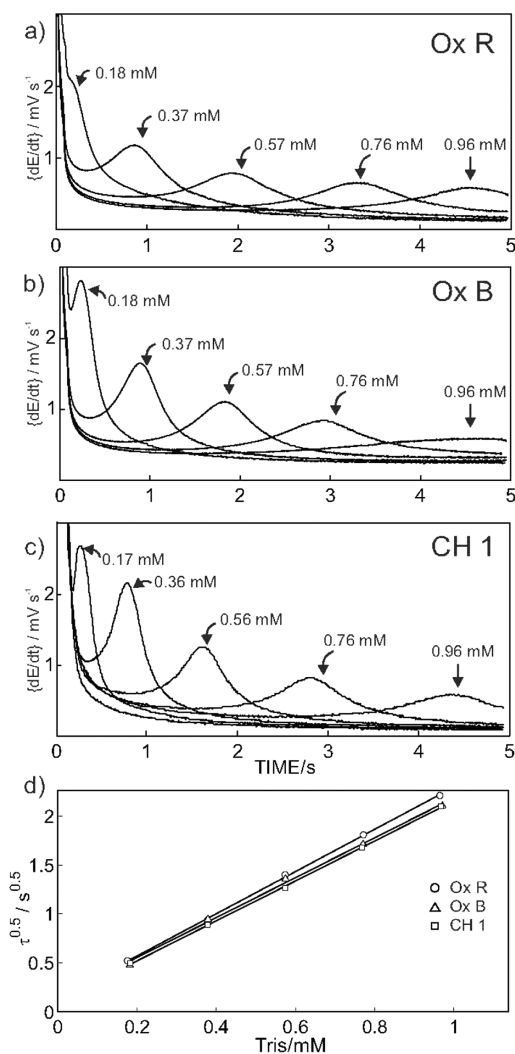


Figure 5. Time derivative of the chronopotentiometric response in contact with a sample containing 0.1 to 1.0 mM of Tris base for (a) Ox R, (b) Ox B, and (c) CH 1. The transition time increases with increasing Tris concentration, as expected from the Sand equation (eq 1). (d) Square root of the transition time ($\tau^{1/2}$) as a function of Tris concentration for all dyes follows a linear relationship.

when Ox R is used, $(5.89 \pm 0.05) \times 10^{-6} \text{ cm}^2 \text{ s}^{-1}$ for Ox B, and $(5.89 \pm 0.05) \times 10^{-6} \text{ cm}^2 \text{ s}^{-1}$ for CH 1. There is some difference between Ox R and Ox B in terms of diffusion coefficient estimation that may be attributed to experimental variations in the effective membrane area, since only geometric areas were estimated here.

CONCLUSIONS

The H^+ -chromoionophore family for ion-selective sensors has been stagnant and has lacked excitement for many years. The variety of available chromoionophores has unfortunately been quite limited for practical applications. A family of fluorescent turn-on oxazinoindoline dyes have been introduced here that exhibit a tunable absorbance, fluorescence, and pK_a values and that will expand the palette of available chromoionophores. Their pH response was characterized by potentiometry and fluorescence spectrometry, and their basicity values compared with CH 1. When used in optical mode, most dyes showed higher basicity than CH 1, while in ISEs, the pK_a values were smaller. This surprising observation was qualitatively explained

by an additional thermal isomerization reaction of the Ox dyes. As a more practical example, a Na^+ -selective optode was successfully prepared and characterized. Compared with the established Nile blue derivatives, the Ox dyes showed a better signal-to-noise ratio when the emission maxima were used as signal output, since they are H^+ turn-on chromoionophores. The compounds were also tested in chronopotentiometry and shown to function without obvious limitation in dynamic electrochemical detection protocols as well.

ASSOCIATED CONTENT

Supporting Information

Synthetic procedures and structural information, fluorescence, and absorbance spectra in membranes and MeCN, pH response for Celgard-based electrodes, calibration for Na^+ -selective optode, optode response for pH-sensitive membrane using DOS as plasticizer, derivation of equations, raw data for Na^+ -selective optode, and chronopotentiometry measurements. This material is available free of charge via the Internet at <http://pubs.acs.org>.

AUTHOR INFORMATION

Corresponding Author

*E-mail: eric.bakker@unige.ch.

Notes

The authors declare no competing financial interest.

ACKNOWLEDGMENTS

The authors thank the Swiss National Science Foundation and University of Geneva for financial support.

REFERENCES

- (1) Dubach, J. M.; Harjes, D. I.; Clark, H. A. *J. Am. Chem. Soc.* **2007**, *129*, 8418.
- (2) Xu, C.; Wygladacz, K.; Retter, R.; Bell, M.; Bakker, E. *Anal. Chem.* **2007**, *79*, 9505.
- (3) Dürüst, N.; Meyerhoff, M. E.; Ünal, N.; Naç, S. *Anal. Chim. Acta* **2011**, *699*, 107.
- (4) Xie, L.; Qin, Y.; Chen, H.-Y. *Anal. Chem.* **2012**, *84*, 1969.
- (5) Bakker, E.; Bühlmann, P.; Pretsch, E. *Chem. Rev.* **1997**, *97*, 3083.
- (6) Bakker, E.; Lerchi, M.; Rosatzin, T.; Rusterholz, B.; Simon, W. *Anal. Chim. Acta* **1993**, *278*, 211.
- (7) Bühlmann, P.; Pretsch, E.; Bakker, E. *Chem. Rev.* **1998**, *98*, 1593.
- (8) Morf, W. E.; Seiler, K.; Rusterholz, B.; Simon, W. *Anal. Chem.* **1990**, *62*, 738.
- (9) Cosofret, V. V.; Nahir, T. M.; Lindner, E.; Buck, R. P. *J. Electroanal. Chem.* **1992**, *327*, 137.
- (10) Wang, K.; Seiler, K.; Morf, W. E.; Spichiger, U. E.; Simon, W.; Lindner, E.; Pungor, E. *Anal. Sci.* **1990**, *6*, 715.
- (11) Lerchi, M.; Bakker, E.; Rusterholz, B.; Simon, W. *Anal. Chem.* **1992**, *64*, 1534.
- (12) Seiler, K.; Morf, W. E.; Rusterholz, B.; Simon, W. *Anal. Sci.* **1989**, *5*, 557.
- (13) Qin, Y.; Bakker, E. *Talanta* **2002**, *58*, 909.
- (14) Ortuño, J. A.; Albero, M. I.; García, M. S.; Garica, M. I.; Expósito, R.; Sánchez-Pedreño, C. *Talanta* **2003**, *60*, 563.
- (15) Badr, I. H.; Meyerhoff, M. E. *J. Am. Chem. Soc.* **2005**, *127*, 5318.
- (16) Mohr, G. J.; Klimant, I.; Spichiger-Keller, U. E.; Wolfbeis, O. S. *Anal. Chem.* **2001**, *73*, 1053.
- (17) Xie, X.; Pawlak, M.; Tercier-Waeber, M.-L.; Bakker, E. *Anal. Chem.* **2012**, *84*, 3163.
- (18) Yu, Z.; Ho, L. Y.; Lin, Q. *J. Am. Chem. Soc.* **2011**, *133*, 11912.
- (19) Huang, D.; Niu, C.; Wang, X.; Lv, X.; Zeng, G. *Anal. Chem.* **2013**, *85*, 1164.
- (20) Wang, J.; Ha, C.-S. *Tetrahedron* **2009**, *65*, 6959.

- (21) Ojida, A.; Takashima, I.; Kohira, T.; Nonaka, H.; Hamachi, I. *J. Am. Chem. Soc.* **2008**, *130*, 12095.
- (22) Li, M.; Lu, H.-Y.; Liu, R.-L.; Chen, J.-D.; Chen, C.-F. *J. Org. Chem.* **2012**, *77*, 3670.
- (23) Ma, X.; Song, F.; Wang, L.; Cheng, Y.; Zhu, C. *J. Polym. Sci., Part A: Polym. Chem.* **2011**, *50*, 517.
- (24) Ma, B.; Wu, S.; Zeng, F. *Sens. Actuators, B* **2010**, *145*, 451.
- (25) Fries, K. H.; Driskell, J. D.; Samanta, S.; Locklin, J. *Anal. Chem.* **2010**, *82*, 3306.
- (26) Tomasulo, M.; Sortino, S.; White, A. J. P.; Raymo, F. M. *J. Org. Chem.* **2005**, *70*, 8180.
- (27) Petersen, M. Å.; Deniz, E.; Nielsen, M. B.; Sortino, S.; Raymo, F. M. *Eur. J. Org. Chem.* **2009**, 4333.
- (28) Deniz, E.; Tomasulo, M.; Cusido, J.; Yildiz, I.; Petriella, M.; Bossi, M. L.; Sortino, S.; Raymo, F. i. M. *J. Phys. Chem. C* **2012**, *116*, 6058.
- (29) Tomasulo, M.; Sortino, S.; Raymo, F. i. M. *J. Photochem. Photobiol., A* **2008**, *200*, 44.
- (30) Xie, X.; Pawlak, M.; Tercier-Waeber, M.-L.; Bakker, E. *Anal. Chem.* **2012**, *84*, 3163.
- (31) Shiraiishi, Y.; Inoue, T.; Sumiya, S.; Hirai, T. *J. Phys. Chem. A* **2011**, *115*, 9083.
- (32) Crespo, G. A.; Afshar, M. G.; Bakker, E. *Anal. Chem.* **2012**, *84*, 10165.
- (33) Shvarev, A.; Bakker, E. *Anal. Chem.* **2003**, *75*, 4541.